



Published in final edited form as:

*Biomacromolecules*. 2010 June 14; 11(6): 1429–1436. doi:10.1021/bm901378a.

## Multivalent Protein Polymer MRI Contrast Agents: Controlling Relaxivity via Modulation of Amino Acid Sequence

Lindsay S. Karfeld-Sulzer, Emily A. Waters, Nicolynn E. Davis<sup>§</sup>, Thomas J. Meade<sup>\*</sup>, and Annelise E. Barron<sup>\*,§</sup>

Departments of Chemical and Biological Engineering, Chemistry, Biochemistry, Molecular Biology, and Cell Biology, Neurobiology and Physiology, and Radiology, Northwestern University, 2145, Sheridan Road, Evanston, IL 60208-3113

### Abstract

Magnetic Resonance Imaging (MRI) is a noninvasive imaging modality with high spatial and temporal resolution. Contrast agents (CAs) are frequently used to increase the contrast between tissues of interest. To increase the effectiveness of MR agents, small molecule CAs have been attached to macromolecules. We have created a family of biodegradable, macromolecular CAs based on protein polymers, allowing control over the CA properties. The protein polymers are monodisperse, random coil, and contain evenly spaced lysines that serve as reactive sites for Gd(III) chelates. The exact sequence and length of the protein can be specified, enabling controlled variation in lysine spacing and molecular weight. Relaxivity could be modulated by changing protein polymer length and lysine spacing. Relaxivities of up to  $\sim 14 \text{ mM}^{-1}\text{s}^{-1}$  per Gd(III) and  $\sim 461 \text{ mM}^{-1}\text{s}^{-1}$  per conjugate were observed. These CAs are biodegradable by incubation with plasmin, such that they can be easily excreted after use. They do not reduce cell viability, a prerequisite for future *in vivo* studies. The protein polymer CAs can be customized for different clinical diagnostic applications, including biomaterial tracking, as a balanced agent with high relaxivity and appropriate molar mass.

### Keywords

Magnetic Resonance Imaging; gadolinium; contrast agent; protein polymer

### Introduction

Engineered biomaterials have been developed for degradable hydrogels and advanced drug delivery, but to fully assess their effectiveness, there is a need to track their fate *in vivo*, noninvasively. Magnetic Resonance Imaging (MRI), with its high temporal and spatial resolution, high soft tissue contrast, and favorable safety profile, is an excellent imaging modality for repeated noninvasive assessment of biomaterials *in vivo*.<sup>1</sup> Contrast agents (CAs), which increase the relaxation rate of water molecules and can help to increase the contrast between tissues of interest, are widely used in experimental and clinical settings.<sup>2</sup> Similarly, CAs incorporated into biomaterials can distinguish their location from surrounding tissues.

<sup>\*</sup>Corresponding authors: Annelise E. Barron: Phone: (650) 721-1151. Fax: (650) 723-9801. aebarron@stanford.edu. Thomas J. Meade: Phone (847) 491-2481. Fax: (847) 491-3832. tmeade@northwestern.edu. Current address: Stanford University, Department of Bioengineering, 318 Campus Drive, W300B James H. Clark Center, Stanford, CA 94305-5440.

Supporting Information **Available**. We provide additional data on the effect of pH on conjugation, cation exchange chromatography and MALDI-TOF data, protein degradation by trypsin, and mammalian cell viability at multiple time points. This information is available free of charge via the Internet at <http://pubs.acs.org/>.

Clinically used CAs based on gadolinium [Gd(III)] are comprised of a Gd(III) ion chelated by a small organic molecule (to reduce the toxicity associated with the free Gd(III) ion),<sup>3</sup> but are not optimized to generate maximum contrast.

The efficiency of a MRI CA at relaxing surrounding protons is given by its relaxivity, which describes the change in relaxation rate in the surrounding protons per unit of agent concentration.<sup>4</sup> According to Solomon-Bloembergen-Morgan theory, three variables are the main contributors to relaxivity:  $\tau_R$ , the rotational correlation time (related to the tumbling rate of the molecule);  $q$ , the number of water molecules bound to each Gd(III) ion; and  $\tau_M$ , the time each water molecule spends bound to the metal ion.<sup>4</sup> At clinical magnetic field strengths,  $\tau_R$  dominates relaxation rates.<sup>5</sup>

Numerous research groups have focused on macromolecular CAs to produce a high molar mass conjugate with multiple Gd(III) ions attached.<sup>3</sup> The large size of these CAs slows molecular tumbling, increasing  $\tau_R$  and hence yielding a higher relaxivity. The presence of multiple Gd(III) ions per molecule increases the local Gd(III) concentration. Previously reported macromolecular CAs include synthetic linear and branched polymers,<sup>6-10</sup> proteins,<sup>11, 12</sup> polysaccharides,<sup>13</sup> viral capsids,<sup>14, 15</sup> nanoparticles,<sup>16, 17</sup> and liposomes.<sup>18</sup> While these macromolecular agents have increased relaxivity compared to small-molecule CAs, a number of limitations remain. Polydispersity is a major disadvantage of modified synthetic polymers and polysaccharides (*e.g.*, dextran).<sup>19</sup> In dynamic contrast-enhanced MRI, CA polydispersity complicates analysis of permeability and makes comparisons unreliable.<sup>20</sup> The large size of viral capsids and nanoparticles can result in greater diffusion barriers and higher likelihood of immune response.<sup>21, 22</sup> In some applications, macromolecular agents with intermediate molecular weights are required, such as in imaging angiogenesis, where it is important to visualize small-diameter blood vessels.<sup>23</sup>

An additional drawback of most macromolecular CAs is that they are not biodegradable. This creates concern since molecules greater than 69 kDa typically are too large to be eliminated through renal glomerular filtration,<sup>24</sup> and some studies have shown that macromolecular CAs are not entirely cleared.<sup>11, 25</sup> A longer *in vivo* residence time allows an extended period for metal-chelator dissociation and may increase the likelihood that the agent will leach Gd(III) ions.

Biodegradable macromolecular CAs offer enhanced contrast and circulation time, while degrading into safely excretable molecules within an appropriate time window. Lu and co-workers have created a series of macromolecular CAs with a cleavable disulfide linker that is broken down by endogenous thiols such as cysteine and glutathione.<sup>10, 26-29</sup> Despite the addition of polyethylene glycol and structural changes to sterically hinder the disulfide bond, these CAs degraded rapidly, resulting in significantly lower MR signal intensity 30 minutes after injection.<sup>27, 30</sup>

We have developed an alternative to synthetic or natural polymers in the form of biodegradable, multivalent, macromolecular CAs based on protein polymers. Genetically engineered and recombinantly expressed protein polymers consist of a repeated amino acid monomer unit.<sup>31</sup> The DNA template from which the bacterial host synthesizes the protein can be precisely specified through cloning techniques. The resulting bacterially expressed, affinity-purified protein polymers are monodisperse, biodegradable, and precisely controlled in terms of sequence, stereochemistry, length, and fold, all favorable properties for CAs. Previously, we have demonstrated the use of lysine-containing, random-coil protein polymers as scaffolding substrates for the conjugation and presentation of various biologically active moieties.<sup>32</sup> We illustrated the flexibility of this protein polymer scaffolding system, by demonstrating the

creation of various bioconjugate constructs with differing reactive site spacing and protein length.

Here, we make use of different, specified protein sequences and lengths, in order to investigate further the properties of a family of previously reported protein polymer-based MRI contrast agents that can be used to track hydrogel degradation, among other applications.<sup>33</sup> Specifically, we analyze the effects of varying the lysine spacing and protein molar mass on the properties (particularly relaxivity) of a contrast agent with Gd(III) chelators conjugated onto some fraction of the lysines that are evenly spaced with the protein polymer. We show that both the protein's molar mass and the lysine spacing affect relaxivity, and we attribute this observation to changes in the rotational correlation time,  $\tau_R$ , of the bioconjugates. Further, we show that these agents are biodegradable, and non-toxic to cells. Our results indicate that the protein polymer contrast agents (PPCAs) described herein can be precisely tuned, in order to create customizable CAs for clinical needs, and moreover, have the capacity for further functionalization and incorporation of bioactive moieties.

## Experimental Methods

### Materials

Unless otherwise stated, all chemicals are purchased from Sigma-Aldrich, Inc. (St. Louis, MO).

### Protein Production

Concatenated DNA templates and the corresponding protein polymers were obtained as described previously.<sup>32</sup> Briefly, the genes encoding the protein polymers were constructed using the controlled cloning method<sup>34</sup> and inserted into modified pET-19b (Novagen, Gibbstown, NJ) plasmids, which then were transformed into BLR(DE3) (Novagen) cells. Cells were cultured in Terrific Broth (Novagen), and the protein was harvested after 4 hours by centrifugation. The protein polymers were purified with affinity chromatography using Chelating Sepharose Fast Flow nickel-charged resin (GE Healthcare, Piscataway, NJ), under denaturing conditions, with competitive elution using imidazole (Fisher Scientific). SDS-PAGE analysis was used to identify the elution fractions containing protein, and these fractions were first dialyzed against distilled, deionized water, and then lyophilized. The molar mass of the protein polymers was determined, and confirmed to match the expected molar mass based on the original gene that was expressed, using matrix-assisted laser desorption ionization time of flight mass spectrometry (MALDI-TOF MS) on a Perseptive Biosystems Voyager Pro DE at Northwestern University's Integrated Molecular Structure Education and Research Center (IMSERC). A 10 mg/mL sinapinic acid matrix in 50% acetonitrile with 0.1% trifluoroacetic acid (TFA) was used.

The protein polymers include a 10× histidine tag (GH<sub>10</sub>SSGHIDDDDKHM) and the amino acid sequences are as follows where n is the number of repeats of the monomer unit in parentheses. The number of monomer repeats ranges from 30 to 120:

K4: GH<sub>10</sub>SSGHIDDDDKHM(GKGSKGGA)<sub>n</sub>G

K6: GH<sub>10</sub>SSGHIDDDDKHM(GKGTGA)<sub>n</sub>G

K8: GH<sub>10</sub>SSGHIDDDDKHM(GKAGTGSA)<sub>n</sub>G

By naming convention, we use the lysine spacing followed by the number of repeats in the format Kx-n, *e.g.* K8-120 for the protein with 120 repeats of the sequence that contains lysines spaced eight amino acids apart.

## Contrast Agent Conjugation and Characterization

Gd(III) chelators were conjugated to lysine-containing protein polymers using a protocol similar to literature procedures, but slightly modified.<sup>33</sup> The protein polymer was dissolved in 0.1 M 4-morpholineethanesulfonic acid (MES) at 1 mg/mL. A 2× molar excess of Gd(III)-\_1,4,7-tris(carboxymethyl)-10-carboxybutyl-1,4,7,10-tetraazacyclododecane [Gd(III)-DO3A], was used with ~29× molar excess of 1-ethyl-3-carbodiimide hydrochloride (EDC, Fisher Scientific) and ~29× molar excess of *N*-hydroxysulfosuccinimide (sulfo-NHS, Fisher Scientific). After initial optimization, the pH of the solution was adjusted to 6.5. The reaction was allowed to proceed for 24 hours, and then the solution was dialyzed against distilled, deionized water inside regenerated cellulose Spectra/Por tubing with a 12-14 kDa molar mass cutoff (Fisher Scientific) for ~48 hours. MALDI-TOF was used, then, to determine the average number of Gd(III) chelators conjugated to the protein polymer, using a sinipinic acid matrix dissolved in 50:50 acetonitrile:water. The protein polymer molar mass was subtracted from the conjugate's molar mass, and divided by the known Gd(III)-DO3A chelator molar mass (585.6 g/mol) to obtain the average degree of valency. Conjugation efficiency, as a percentage, is defined as the number of Gd(III)-DO3A conjugates on a PPCA divided by the total number of reactive lysine sites, multiplied by 100.

The K8-30 CA was analyzed as well by cation exchange chromatography on an FPLC system with FPLC Director software (GE Healthcare), at Ohmx Corporation. The CA was dissolved at 2 mg/mL in 20 mM sodium citrate, pH 2.6 buffer, and then filtered with a 0.2 μm syringe filter prior to injection onto the FPLC system. A mono S HR 5/5 column (GE Healthcare) was used with a gradient buffer system of consisting of A: 20 mM sodium citrate, pH 2.6 buffer, and B: with 2 M NaCl. After washing steps, a linear gradient of NaCl salt concentration, from 0 to 2 M NaCl over 20 minutes, was employed to elute the PPCA from the column. Protein concentration was determined by monitoring the UV absorbance at 254 and 280 nm. MALDI-TOF was used to determine the molar mass of the compound in each of the fractions. The polydispersity index (PDI) of the protein sample was estimated by use of the peak in signal intensity data obtained in the MALDI analysis, and using the standard equations for the weight-average molar mass and the number-average molar mass.<sup>35</sup>

## Relaxivity

$T_1$  measurements were performed in triplicate using a Bruker mq60 NMR Analyzer (Bruker Canada, Milton, Ont., Canada) at 60 MHz (1.5 T) and 37 °C, at three concentrations. For each PPCA, the relaxivity was determined independently for three different batches of CAs that had been synthesized under the same conditions. Inductively coupled plasma atomic emission spectrometry (ICP-AES) was performed on a Varian VISTA-MPX ICP spectrometer (Palo Alto, CA) at Northwestern University's IMSERC, and was used to estimate the Gd(III) concentration in a given mass of protein-based CA. Relaxivity was determined by calculating the slope of  $1/T_1$  versus Gd(III) concentration. The data are reported as the mean ± standard deviation, using the results obtained for three different batches.

## Phantom Images

K8-120 PPCA samples were prepared at different concentrations in a solution containing unmodified protein polymers at 9.4 wt% total protein polymer with 0.75 mM ethylenediaminetetraacetic acid (EDTA), 75 mM 4-Morpholinepropanesulfonic acid (MOPS), and 7.5 mM CaCl<sub>2</sub>. Samples were imaged using a 4.7 T Bruker Biospec 4740 MR imager at Northshore University HealthSystem Research Institute using a volume coil without temperature control. A spin echo pulse sequence of TR = 350 ms, TE = 14.5 ms, 4 signal averages, and a 0.12 × 0.12 × 1 mm<sup>3</sup> resolution was used. To calculate  $T_1$ s, a spin echo pulse sequence with multiple TRs was used with TE = 12.5 ms, TR = 100, 225, 350, 500, 675, 900, 1175, 1575, 2250, and 5000 ms, two signal averages, and a 0.12 × 0.12 × 1 mm<sup>3</sup> resolution.

$T_2$  values were measured using a multiecho sequence with TR = 3000 ms, TE = 20 ms, then every 20 ms through 640 ms, two signal averages and a  $0.12 \times 0.12 \times 1 \text{ mm}^3$  resolution. Data were fit in Origin 7 (OriginLab Corporation, Northampton, MA) with a nonlinear curve-fitting function, using the following equations:

$$S_{TRi} = S_{TR0} (1 - \exp(-TR / T_1)) \quad (1)$$

$$S_{TEi} = S_{TE0} \exp(-TE / T_2) \quad (2)$$

where  $S_{TR0}$  and  $S_{TE0}$  are constants,  $S_{TRi}$  is the signal intensity at a particular TR, and  $S_{TEi}$  is the signal intensity at a particular TE. Regions of interest (ROI) were defined and average signal intensities across the ROIs were used in the curve fitting equations.  $T_1$  and  $T_2$  are reported as the value and standard deviation as determined from the curve fitting. After imaging, the Gd(III) concentration in the samples was analyzed by inductively coupled plasma mass spectrometry (ICP-MS) on a Thermo Electron Corporation (Waltham, MA) XSeriesII ICP-MS with Thermo PlasmaLab software. All Gd(III) standards and samples contained 5 ng/mL of a multi-element internal standard (Spex CertiPrep, Metuchen, NJ) consisting of Bi, Ho, In, Li, Sc, Tb, Y, and 3% nitric acid (v/v).

### Biodegradation

PPCAs were dissolved in 20 mM Tris, 150 mM NaCl, pH 7.5 buffer at 1.6 mg/mL. Plasmin was dissolved in the same buffer at 0.5 units/mL. The CAs were incubated with an equal volume of plasmin solution, or alone in a 37 °C incubator. Aliquots were removed at 3, 6, and 24 hours, immediately frozen with liquid nitrogen to inactivate the enzyme, and then stored at -20 °C until further use. To assess degradation, the samples were boiled for 7 minutes with 1% (w/v) sodium dodecyl sulfate (SDS) and monitored by electrophoretic methods on a 12% SDS polyacrylamide gel (SDS-PAGE).

### Cell Culture and Viability

MIN6 cells were cultured in DMEM containing 4.5 g/L glucose and L-glutamine, 3.4 g/L sodium bicarbonate, 5  $\mu\text{L/L}$   $\beta$ -mercaptoethanol, 75 mg/L penicillin, 50 mg/L streptomycin, and 15% fetal bovine serum in a humidified incubator at 37 °C and 5%  $\text{CO}_2$ . Cells were plated in 24-well plates such that they reached approximately 80% confluency after growing overnight. PPCAs were dissolved in cell culture media and filtered with a 0.2  $\mu\text{m}$  filter as a sterilization method. This stock solution was created at concentrations that we expected should yield a Gd(III) concentration of around 2 mM, but debris and weighing error may cause inaccuracy. The contrast agent stock was reserved for Gd(III) concentration measurement with ICP-MS on a computer-controlled Thermo Elemental (Waltham, MA) PQ ExCell inductively coupled plasma mass spectrometer. In addition to the stock solution concentration, two other concentrations were created by diluting the stock solution by 1/3 and 2/3 with culture media. The cells were incubated for five hours with the three concentrations of contrast agent (total of 400  $\mu\text{L}$  in each well) and each concentration was performed in triplicate.

After incubation with the contrast agent, the cell culture media was removed, and the cell monolayer was gently rinsed with phosphate buffered saline (PBS). 0.2  $\mu\text{L}$  of trypsin solution was added to each well and the plate was placed in the incubator for 1 – 5 minutes to allow the

trypsin to detach the cells from the plate. Cells were suspended and placed into 1.5-mL microcentrifuge tubes. 20  $\mu$ L of the cell suspension was combined with 180  $\mu$ L of Guava ViaCount reagent (Guava Technologies, Hayward, CA), vortexed, and incubated at room temperature for five minutes. The Guava ViaCount Assay was then performed on the Guava EasyCite Mini Personal Cell Analyzer to obtain cell count and cell viability. The data are reported as the mean  $\pm$  standard deviation for the three samples.

### Statistical Analysis

Statistics were performed using Origin 7 (OriginLab Corporation, Northampton, MA) with a one-tailed, two-sample T test and a significance level of 0.05.

## Results

### Contrast Agent Synthesis and Characterization

Protein polymer contrast agents were synthesized using five different protein polymers: K8-30, K8-60, K8-120 (which comprise 30, 60, and 120 repeats, respectively, of the amino acid sequence GKAGTGSA); K4-30 (30 repeats of GKGSGKGA), and K6-40 (40 repeats of GKGTGA) (see Figure 1). The pH of the aqueous reaction solution that was used to conjugate the Gd(III) DO3A chelators to the lysines in the protein polymers was optimized, initially, using K8-30 protein. The number of Gd(III) chelators attached to the protein polymer was significantly higher at pH 6 and 7 than at pH 5 or 7.5 (Figure S1). In all subsequent reactions, a pH of 6.5 was used. With this synthetic methodology, the conjugation efficiency was consistent with all of the protein polymers, and ranged from 23.2% to 28.0% (Tables 1 and 2). Cation exchange chromatography revealed that the K8-30 PPCA eluted in a single peak, less than one minute wide (Figure S2A). MALDI analysis of the corresponding fractions indicated that the conjugate was present. We estimated a weight-average molar mass of 27,384 Da, and a number-average molar mass of 27,299 Da, which yields an estimated polydispersity index is 1.003 (Figure S2B).

### Contrast Agent Relaxivity

The  $T_1$  was measured at 60 MHz and 37  $^{\circ}$ C for a range of Gd(III) concentrations, to allow the calculation of  $T_1$  relaxivities (measured by ICP-AES). The relaxivity per Gd(III) increased with the number of monomer repeats, as demonstrated when comparing K8-30, K8-60, and K8-120 (Table 1 and Figure 2). Lysines were spaced eight amino acids apart, while the molar mass of the protein polymer varied from 21.7 kDa to 78.4 kDa. The relaxivity per Gd(III) of K8-120 CA is the highest at 14.6  $\text{mM}^{-1}\text{s}^{-1}$ , which is statistically significant compared to the K8-30 and K8-60 CAs ( $P < 0.01$ ). This relaxivity value is about 3-5 times higher than that for clinically used small-molecule contrast agents such as 1,4,7,10-tetraaza cyclododecane-1,4,7,10-tetraacetic acid (DOTA) or diethylenetriaminopentaacetic acid (DTPA).<sup>36</sup> We found total relaxivities per CA molecule that were as high as 461.4  $\text{mM}^{-1}\text{s}^{-1}$ , with approximately 32 Gd(III) chelates attached to the K8-120 protein polymer.

The relaxivities were compared between protein polymer CAs that had similar molar masses, but different lysine spacing along the backbone. We obtained a significantly higher value of the relaxivity per Gd(III) for the protein polymer CA with the closest lysine spacing (four amino acids apart,  $P < 0.01$ ) (see Table 2 and Figure 3). The relaxivities per Gd(III) that we measured averaged 12.1  $\text{mM}^{-1}\text{s}^{-1}$ , 9.1  $\text{mM}^{-1}\text{s}^{-1}$ , and 8.8  $\text{mM}^{-1}\text{s}^{-1}$  for K4-30, K6-40, and K8-30, respectively.

## MR Images

To create solution phantoms for MR imaging, K8-120 PPCA was prepared in a mixture of unmodified protein polymers. As shown in Figure 4, there is a significant contrast enhancement as the Gd(III) concentration increases from 0.0 mM to 0.37 mM and in the absence of Gd(III), the protein polymer sample is brighter than water. At the highest Gd(III) concentration,  $T_1$  is 3.3 times lower and  $T_2$  is 2.7 times lower than the values without Gd(III) (Table 3). As indicated by the ratio of  $T_1/T_2$ , there is proportionally less  $T_2$  shortening at the highest concentration.

## Biodegradation of the Protein Polymer Contrast Agents

All three of the PPCAs tested (K8-30, K8-60, and K8-120) were biodegradable by plasmin, a naturally occurring enzyme that cleaves on the carboxyl side of lysine residues (Figure 5). When the PPCAs were incubated with plasmin, the intensity of the band demarcating the full-length contrast agent decreased over time, showing degradation of the PPCA. In the absence of plasmin, the intensity of the band remained approximately constant, indicating that plasmin is performing the digestion. While it has been shown prior to this that the protein polymers can be degraded by plasmin,<sup>32</sup> it was unknown whether or not derivatizing the protein polymer with Gd(III) chelators would inhibit protease action.

These data indicate that degradation occurs, even with the modification of ~25% of the lysines. It is unclear whether plasmin can recognize the modified lysines for digestion, or if it only cleaves next to the unmodified lysines. The SDS-PAGE results do not entirely explain the mechanism, as there are no distinct bands observed, other than the band for the full-length PPCA, with the others appearing as a “smear”. This could be due to either 1) degradation into very small pieces that are too small for SDS-PAGE detection, or 2) low enough concentrations at each molar mass such that they are not detected as distinct bands.

## Cell Viability in the Presence of Protein Polymer Contrast Agents

The viability of MIN6 cells incubated with PPCAs for five hours was tested using a Guava Viacount Assay. For CAs with each of the three protein lengths containing lysines spaced eight amino acids apart, the viability was greater than 90% (Figure 6). For Gd(III) concentrations up to 2.1 mM, viability ranged between 93% and 97%. Preliminary data with cells incubated with K8-30 CA for up to 48 hours showed similar results (Figure S3). It is not expected that higher concentrations would be needed for *in vivo* applications. Highly cationic proteins and polymers have been previously shown to be cytotoxic,<sup>37</sup> but the density of the lysines in these PPCAs appears to be low enough to avoid harmful effects (~25% are modified with a Gd(III) chelator).

## Discussion

We have developed a family of high-relaxivity, multivalent bioconjugates through the aqueous chemical linking of DO3A-based Gd(III) chelators to lysine-containing, random-coil protein polymers. The monodisperse nature of genetically engineered, recombinantly expressed protein polymers enables us to explore the effect of varying the polymer sequence and length on its relaxometric properties. Furthermore, we have shown that these CAs are biodegradable and non-toxic, as essential for progression to *in vivo* studies.

The protein polymers used in the construction of the PPCAs were chosen as a means to study the impact of the lysine spacing, while maintaining stable constructs. The protein sequence itself was designed to minimize protein-protein interactions through sequence and secondary structure and maintain solubility and stability. As shown previously, these protein polymers adopt random coil configurations in aqueous solution, and have high water solubilities over a wide range of temperatures.<sup>32</sup> We designed the sequence to favor the tendency for a random-

coil configuration to be adopted, by avoiding the inclusion of hydrophobic amino acids completely, and including only positively charged amino acids (which repel each other ionically). We hypothesized that more complex amino acid sequences would be more likely to adopt other secondary structures such as  $\alpha$ -helix and  $\beta$ -sheet, at least locally, in which case the protein might collapse into a more dense configuration in water overall, which would lead to a decreased rotational correlation time or otherwise influence relaxivity and solubility.

PPCAs were synthesized in aqueous solution by amide bond formation between the primary amine on the lysine residues and the free carboxyl group on the Gd(III)-DO3A chelator. It was necessary to optimize the pH in the coupling reaction to maximize conjugation efficiency in the one pot reaction. The amide bond formation reaction with Sulfo-NHS and EDC is a three step process.<sup>38</sup> In the first step, an unstable reactive *O*-acylisourea ester intermediate is formed with the reaction of the EDC with the carboxyl group. Subsequently, the Sulfo-NHS group reacts with this intermediate to form a semi-stable amine-reactive NHS ester. Lastly, the primary amine reacts with the semi-stable NHS ester to form a stable amide bond. The optimal pH of these reactions varies, with the NHS ester more stable at a lower pH (4.7 – 6.0), while at a higher pH, the amine is more nucleophilic, and thus more reactive. An intermediate pH is necessary to obtain maximal conversion. The conversion of this reaction is inherently limited since the unstable reactive *O*-acylisourea ester intermediate can be hydrolyzed to return the initial carboxyl moiety; therefore, the yield of amide bond formation in water will be much lower than in anhydrous organic solvents. Since the protein polymers are not soluble in organic solvents, amide bond formation is limited to aqueous conjugation.

As discussed earlier, increasing the rotational correlation time,  $\tau_R$ , significantly increases the relaxivity at low magnetic fields.<sup>3</sup> We believe that the increase in relaxivity per Gd(III) with higher molecular weight protein polymer backbones is due to a longer rotational correlation time.<sup>3</sup> As previously described by Caravan et al., attaching small Gd(III) chelators to proteins slows tumbling to increase relaxivity.<sup>39</sup> Other modes of rotation can decrease the impact of higher molecular weight, such as in linear polylysine where the flexible chains limit effective tumbling speed.<sup>40</sup> However, progressively higher molecular weight proteins with the same protein sequence, as shown here with K8-30, K8-60, and K8-120, should have correspondingly greater rotational correlation times.

The rotational correlation time is a combination of overall molecular tumbling and internal rotational flexibility of the conjugated Gd(III) moiety<sup>41</sup> so internal rotation of attached Gd(III) chelates also plays a critical role.<sup>42</sup> Based on the results of varying lysine spacing, we hypothesize that the four-amino-acid spacing between lysines results in steric hindrance of the Gd(III) chelators, increasing relaxivity. The proteins have a random coil secondary structure, such that the PPCA may take a globular formation where the different sections can come into contact with each other. As indicated in Figure 1, when there is a higher density of lysines, and thus a higher density of Gd(III) chelators, there is a greater probability of the chelators interacting with each other. If the chelators are close enough together, they can limit the flexibility and inhibit full rotation of the molecules to increase relaxivity.

The high relaxivity measured at 1.5 T is apparent on phantoms imaged at 4.7 T (Figure 5). At 0.37 mM Gd(III), the K8-120 CA displays significant contrast over water and the control, despite the somewhat diminished effect of longer rotational correlation times at higher magnetic fields.<sup>41</sup> Although in vivo contrast depends on a number of factors, the relaxation times demonstrated with 0.37 mM Gd(III) of the K8-120 PPCA would most likely be more than sufficient to visualize the area of interest in many tissues. Water and macromolecular content, adjacent fat, and the effective concentration in addition to the relaxivity of the contrast agent all influence the detected contrast. The protein-containing sample without any Gd(III)



likely shows higher signal than water due to  $T_1$  shortening of the water molecules resulting from their interaction with the macromolecular proteins.

Since the protein polymer CAs consist of naturally occurring amino acids, we hypothesized that they would be biodegradable by enzymes. Biodegradation was analyzed by incubating the PPCAs with plasmin, an enzyme naturally present in the blood that cleaves on the carboxyl side of lysine residues. This enzyme is naturally present in the blood and degrades many blood plasma proteins, particularly fibrin. Each of the three lengths of the PPCAs with lysines spaced eight amino acids apart (K8-30, K8-60, and K8-120) was cleaved by plasmin (Figure 6). The increased degradation over time indicates that the enzyme continues to cleave the PPCA, without dependence on length. No full length PPCA remains after 24 hours of incubation. The random coil configuration of the proteins likely provides easier plasmin access than proteins with other types of secondary structure. There may be some interactions between protein polymer strands, but the high stability of the proteins indicates any attractions would be weak. The lower resistance to rearranging conformations would facilitate exposure to enzymes. Although this experiment does not accurately represent an *in vivo* scenario in terms of complexity, the plasmin concentration approximately corresponds to the physiological concentration of its precursor plasminogen in serum.<sup>43</sup> Incubation of the PPCAs with trypsin, a less selective enzyme that cleaves on the carboxyl side of lysine residues, also showed degradation (Figure S3), suggesting potential for degradation by other enzymes as well as through general hydrolysis. With multiple possible routes of degradation, these CAs will likely degrade *in vivo* and be efficiently cleared from the body. These PPCAs may avoid the safety concerns of synthetic macromolecular CAs.

Since these PPCAs degrade, they can be incorporated into degradable hydrogels for fate mapping. Biomaterial degradation is an important parameter in tissue engineering, where ideally a hydrogel degrades at the rate of tissue ingrowth, and in controlled release drug delivery, where the degradation rate determines available drug concentration.<sup>44, 45</sup> We have shown that the PPCAs can be covalently crosslinked into protein polymer hydrogels and demonstrate higher signal than a control without PPCA.<sup>33</sup> Additionally, the remaining free amines are available for crosslinking into other biomaterials with amine-reactive functional groups.

The PPCAs are uniquely positioned for use in contrast-enhanced angiography due to the ability to control the protein polymer length and sequence. Others have shown improved performance of macromolecular contrast media over small molecule CAs, such as Gd(III)-DTPA and Gd(III)-DOTA, in imaging vasculature. Various macromolecular blood pool agents have displayed increased contrast and ability to distinguish blood vessels over small molecule CAs, including albumin-Gd-DTPA, Gadomer, and polydisulfide agents.<sup>46-48</sup> However, larger macromolecular CAs have restricted diffusion that can prevent effective imaging, as shown when comparing a 6.47 kDa CA to a 52 kDa CA.<sup>22</sup> Protein-binding agents are small molecules that have high diffusion, but can bind to proteins such as albumin to increase their relaxivity. Both protein-binding agents B-22956/1 and recently clinically approved MS-325 display increased contrast without restricted diffusion, but they are bound through non-covalent interactions.<sup>49, 50</sup> The PPCAs with covalently attached Gd(III)-DO3A can be synthesized with varying properties to create a balanced agent with high relaxivity and appropriate molecular weight to be customized to different clinical diagnostic applications.

## Conclusion

This new family of protein polymer contrast agents may have the potential to enable *in vivo* biomaterial fate mapping due to its high relaxivity, biodegradability, and apparently low cytotoxicity. As shown here, the relaxivity of the CAs depends on the molar mass and amino

acid sequence of the protein polymer backbone. By the use of monodisperse protein polymers as the scaffolding entities, the properties of these CAs can be controlled, which may favor their eventual clinical use. Furthermore, due to the multivalent nature of the chemically reactive lysine monomers on these PPCAs, they can serve as a useful, general scaffold that can be decorated with a variety of small biological moieties (e.g., polypeptides) to create CAs targeted to certain types of cells or tissues.

## Supplementary Material

Refer to Web version on PubMed Central for supplementary material.

## Acknowledgments

We thank Emily Testa for synthesizing the Gd-DO3A compound, Keith Macrenaris for ICP-MS data acquisition, Ellen Kohlmeir for MIN6 cell culture. We thank the NIH/NIBIB (R01EB003806 and R01EB005866), Northwestern University's NIH/NRSA Biotechnology Training Grant (2-T32-GM008449), and NIH/CCNE (5 U54 CA119341-02) for generous support of this research. We gratefully acknowledge Ohmx Corporation for the helpful discussions and the use of an FPLC system. We thank Northwestern University's Institute for Bionanotechnology in Medicine and Integrated Molecular Structure Education and Research Center for the use of MALDI-TOF and ICP-AES instruments. We thank Northshore University HealthSystem Research Institute for the use of the 4.7 T imager, which has support from NIH/NCRR Grant S10 RR15685-01.

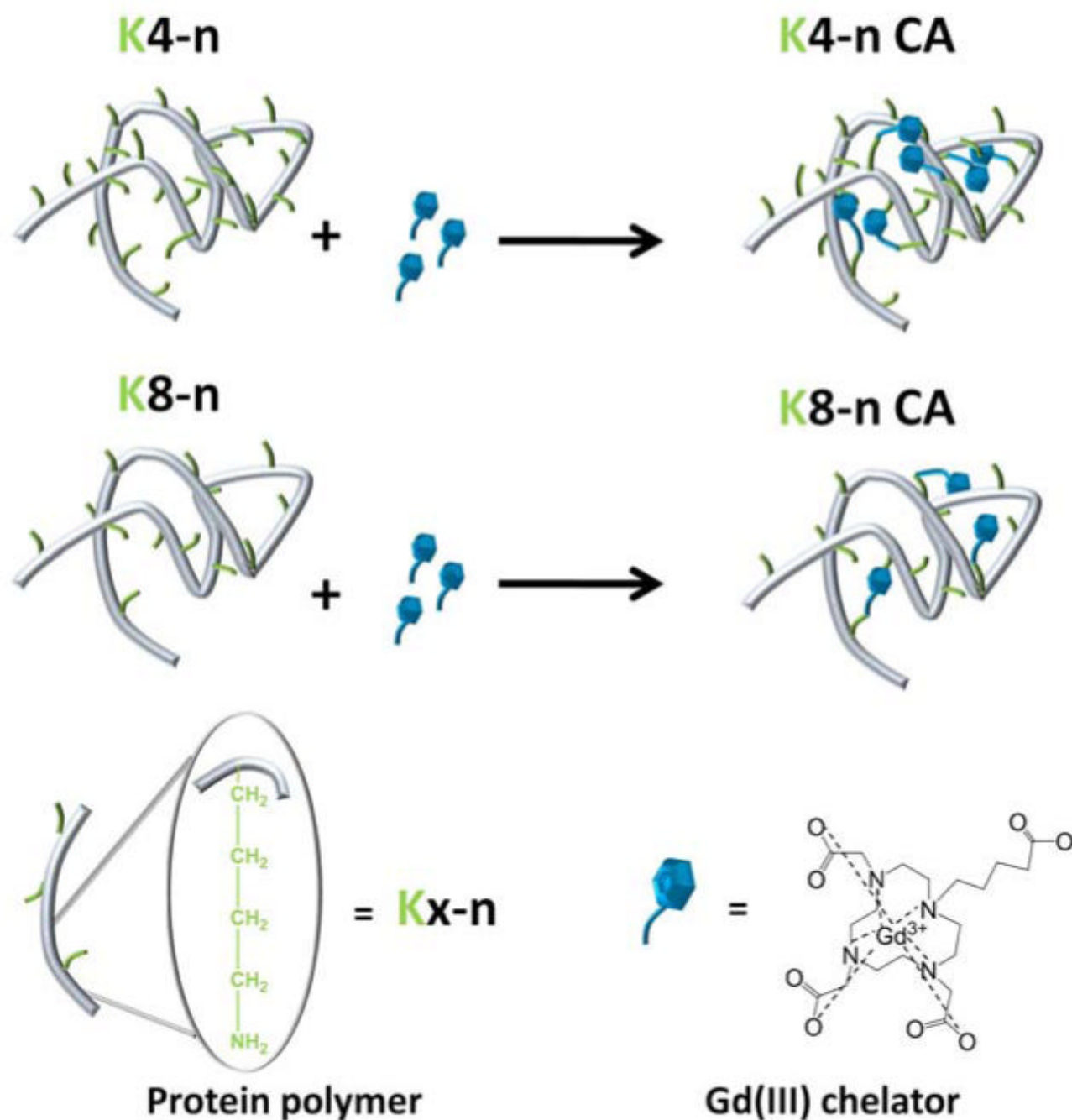
## References

1. Cherry SR. In vivo molecular and genomic imaging: new challenges for imaging physics. *Physics in Medicine and Biology* 2004;49:R13–R48. [PubMed: 15012005]
2. Burns, M. The U.S market for medical imaging contrast media. Bio-tech Systems; Las Vegas, N.V.: 2007.
3. Caravan P, Ellison JJ, McMurry TJ, Lauffer RB. Gadolinium(III) chelates as MRI contrast agents: structure, dynamics, and applications. *Chemical Reviews* 1999;99:2293–2352. [PubMed: 11749483]
4. Merbach, AE.; Toth, E. *The Chemistry of Contrast Agents in Medical Magnetic Resonance Imaging*. John Wiley & Sons, Ltd.; West Sussex, England: 2001.
5. Rudovsky J, Botta M, Hermann P, Hardcastle KI, Lukes I, Aime S. PAMAM dendrimeric conjugates with a Gd-DOTA phosphinate derivative and their adducts with polyaminoacids: The interplay of global motion, internal rotation, and fast water exchange. *Bioconjugate Chemistry* 2006;17(4):975–987. [PubMed: 16848405]
6. Schuhmann-Giampieri G, Schmitt-Willich H, Frenzel T, Press WF, Weinmann HJ. In vivo and in vitro evaluation of Gd-DTPA-polylysine as a macromolecular contrast agent for magnetic resonance imaging. *Investigative Radiology* 1991;26:969–974. [PubMed: 1743920]
7. Wen X, Jackson EF, Price RE, Kim EE, Wu Q, Wallace S, Charnsangavej C, Gelovani JG, Li C. Synthesis and characterization of poly(L-glutamic acid) gadolinium chelate: a new biodegradable MRI contrast agent. *Bioconjugate Chemistry* 2004;15:1408–1415. [PubMed: 15546209]
8. Zhu D, Lu X, Hardy PA, Leggas M, Jay M. Nanotemplate-engineered nanoparticles containing gadolinium for magnetic resonance imaging of tumors. *Investigative Radiology* 2008;43(2):129–140. [PubMed: 18197065]
9. Cyran C, Fu Y, Raatschen HJ, Rogut V, Chaopathomkul B, Shames DM, Wendlend MF, Yeh BM, Brasch RC. New macromolecular polymeric MRI contrast agents for application in the differentiation of cancer from benign soft tissues. *Journal of Magnetic Resonance Imaging* 2008;27:581–589. [PubMed: 18219614]
10. Lu ZR, Parker DL, Goodrich KC, Wang X, Dalle JG, Buswell HR. Extracellular biodegradable macromolecular gadolinium(III) complexes for MRI. *Magnetic Resonance in Medicine* 2004;51:27–34. [PubMed: 14705042]
11. Franano FN, Edwards WB, Welch MJ, Brechbiel MW, Gansow OA, Duncan JR. Biodistribution and metabolism of targeted and nontargeted protein-chelate-gadolinium complexes: Evidence for gadolinium dissociation in vitro and in vivo. *Magnetic Resonance Imaging* 1995;13:201–214. [PubMed: 7739361]

12. Nagaraja TN, Croxen RL, Panda S, Knight RA, Keenan KA, Brown SL, Fenstermaker JD, Ewing JR. Application of arsenazo III in the preparation and characterization of an albumin-linked gadolinium-based macromolecular magnetic resonance contrast agent. *Journal of Neuroscience Methods* 2006;157:238–245. [PubMed: 16769125]
13. Sirlin CB, Vera DR, Corbell JA, Caballero MB, Buxton RB, Mattrey RF. Gadolinium-DTPA-dextran: a macromolecular MR blood pool contrast agent. *Academic Radiology* 2004;11:1361–169. [PubMed: 15596374]
14. Anderson EA, Isaacman S, Peabody DS, Wang EY, Canary JW, Kirshenbaum K. Viral nanoparticles donning a paramagnetic coat: Conjugation of MRI contrast agents to the MS2 capsid. *Nano Letters* 2006;6(6):1160–1164. [PubMed: 16771573]
15. Liepold L, Anderson S, Willits D, Oltrogge L, Frank JA, Douglas T, Young M. Viral capsids as MRI contrast agents. *Magnetic Resonance in Medicine* 2007;58:871–879. [PubMed: 17969126]
16. Alric C, Taleb J, Le Duc G, Mandon C, Billotey C, Le Meur-Herland A, Brochard T, Vocanson F, Janier M, Perriat P, Roux S, Tillement O. Gadolinium chelate coated gold nanoparticles as contrast agents for both x-ray computer tomography and magnetic resonance imaging. *Journal of the American Chemical Society* 2008;130:5908–5915. [PubMed: 18407638]
17. Battistini E, Gianolio E, Gref R, Couvreur P, Fuzerova S, Othman M, Aime S, Badet B, Durand P. High-relaxivity magnetic resonance imaging (MRI) contrast agent based on supramolecular assembly between a gadolinium chelate, a modified dextran, and poly- $\beta$ -cyclodextrin. *Chemistry - A European Journal* 2008;14:4551–4561.
18. Erdogan S, Medarova ZO, Roby A, Moore A, Torchilin VP. Enhanced tumor MR imaging with gadolinium-loaded polychelating polymer-containing tumor-targeted liposomes. *Journal of Magnetic Resonance Imaging* 2008;27:574–580. [PubMed: 18219628]
19. Weinmann H, Ebert W, Misselwitz B, Schmitt-Willich H. Tissue-specific MR contrast agents. *European Journal of Radiology* 2003;46:33–44. [PubMed: 12648800]
20. Barrett T, Brechbiel MW, Bernardo M, Choyke PL. MRI of tumor angiogenesis. *Journal of Magnetic Resonance Imaging* 2007;26(2):235–249. [PubMed: 17623889]
21. Barrett T, Kobayashi H, Brechbiel M, Choyke PL. Macromolecular MRI contrast agents for imaging tumor angiogenesis. *European Journal of Radiology* 2006;60:353–366. [PubMed: 16930905]
22. Watrin-Pinzano A, Loeuille D, Goebel JC, Lapicque F, Walter F, Robert P, Netter P, Corot C, Gillet P, Blum A. Quantitative dynamic contrast enhance MRI of experimental synovitis in the rabbit knee: comparison of macromolecular blood pool agents vs. Gadolinium-DOTA. *Bio-medical materials and engineering* 2008;18(4-5):261–272. [PubMed: 19065032]
23. Oostendorp M, Post MJ, Backes WH. Vessel growth and function: depiction with contrast-enhance MR imaging. *Radiology* 2009;251:317–335. [PubMed: 19401568]
24. Preda A, van Vliet M, Krestin GP, Brasch RC, van Dijke CF. Magnetic resonance macromolecular agents for monitoring tumor microvessels and angiogenesis inhibition. *Investigative Radiology* 2006;41(3):325–331. [PubMed: 16481916]
25. Rebizak R, Schaefer M, Dellacherie E. Polymeric conjugates of Gd(3+)-diethylenetriaminepentaacetic acid and dextran. 2. Influence of spacer arm length and conjugate molecular mass on the paramagnetic properties and some biological parameters. *Bioconjugate Chemistry* 1998;9:94–99. [PubMed: 9460551]
26. Mohs AM, Nguyen T, Jeong EK, Feng Y, Emerson L, Zong Y, Parker DL, Lu ZR. Modification of Gd-DTPA cystine copolymers with PEG-1000 optimizes pharmacokinetics and tissue retention for magnetic resonance angiography. *Magnetic Resonance in Medicine* 2007;58:110–118. [PubMed: 17659618]
27. Mohs A, Wang X, Goodrich K, Zong Y, Parker D, Lu Z. PEG-g-poly(GdDTPA-co-L-cystine): a biodegradable macromolecular blood pool contrast agent for MR imaging. *Bioconjugate Chemistry* 2004;15:1424–1430. [PubMed: 15546211]
28. Wang X, Feng Y, Ke T, Schabel M, Lu Z. Pharmacokinetics and tissue retention of (Gd-DTPA)-cystamine copolymers, a biodegradable macromolecular magnetic resonance imaging contrast agent. *Pharmaceutical Research* 2004;22:596–602. [PubMed: 15846467]

29. Xu R, Wang Y, Wang X, Jeong EK, Parker DL, Lu ZR. In vivo evaluation of a PAMAM-cystamine-(Gd-DO3A) conjugate as a biodegradable macromolecular MRI contrast agent. *Experimental Biology and Medicine* 2007;232(8):1081–1089. [PubMed: 17720954]
30. Zong Y, Wang X, Jeong EK, Parker DL, Lu ZR. Structural effect on degradability and in vivo contrast enhancement of polydisulfide Gd(III) complexes as biodegradable macromolecular MRI contrast agents. *Magnetic Resonance Imaging* 2009;27:503–511. [PubMed: 18814987]
31. Megeed Z, Haider M, Li DQ, O'Malley BW, Cappello J, Ghandehari H. In vitro and in vivo evaluation of recombinant silk-elastinlike hydrogels for cancer gene therapy. *Journal of Controlled Release* 2004;94(2-3):433–445. [PubMed: 14744493]
32. Davis NE, Karfeld-Sulzer LS, Ding S, Barron AE. Synthesis and characterization of a new class of cationic protein polymers for multivalent display and biomaterial applications. *Biomacromolecules* 2009;10(5):1125–1134. [PubMed: 19361214]
33. Karfeld LS, Bull SR, Davis NE, Meade TJ, Barron AE. Use of a genetically engineered protein for the design of a multivalent MRI contrast agent. *Bioconjugate Chemistry* 2007;18:1697–1700. [PubMed: 17927227]
34. Won JI, Barron AE. A new cloning method for the preparation of long repetitive polypeptides without a sequence requirement. *Macromolecules* 2002;35:8281–8287.
35. Fu Y, Raatschen HJ, Nitecki DE, Wendlend MF, Novikov V, Fournier LS, Cyran C, Rogut V, Shames DM, Brasch RC. Cascade polymeric MRI contrast media derived from poly(ethylene glycol) cores: initial syntheses and characterizations. *Biomacromolecules* 2007;8:1519–1529. [PubMed: 17402781]
36. Artemov D, Bhujwala ZM, Bulte JWM. Magnetic resonance imaging of cell surface receptors using targeted contrast agents. *Current Pharmaceutical Biotechnology* 2004;5:485–494. [PubMed: 15579038]
37. Putnam D, Gentry CA, Pack DW, Langer R. Polymer-based gene delivery with low cytotoxicity by a unique balance of side-chain termini. *Proceedings of the National Academy of Sciences* 2001;98(3):1200–1205.
38. Hermanson, GT. *Bioconjugate Chemistry*. Academic Press; San Diego: 1996.
39. Caravan P. Protein-targeted gadolinium-based magnetic resonance imaging (MRI) contrast agents: design and mechanism of action. *Accounts of Chemical Research* 2009;42(7):851–862. [PubMed: 19222207]
40. Spanoghe M, Lanens D, Dommissie R, Van der Linden A, Alderweireldt F. Proton relaxation enhancement by means of serum albumin and poly-L-lysine labeled with DTPA-Gd<sup>3+</sup>: relaxivities as a function of molecular weight and conjugation efficiency. *Magn Reson Imaging* 1992;10(6):913–7. [PubMed: 1334186]
41. Caravan P, Farrar CT, Frullano L, Uppal R. Influence of molecular parameters and increasing magnetic field strength on relaxivity of gadolinium- and manganese-based T1 contrast agents. *Contrast Media and Molecular Imaging* 2009;4:89–100. [PubMed: 19177472]
42. Caravan P. Strategies for increasing the sensitivity of gadolinium based MRI contrast agents. *Chemical Society Reviews* 2006;35:512–523. [PubMed: 16729145]
43. Fuchs H, Wallich R, Simon MM, Kramer MD. The outer surface protein A of the spirochete *Borrelia burgdorferi* is a plasmin(ogen) receptor. *Proc Natl Acad Sci U S A* 1994;91:12594–12598. [PubMed: 7809084]
44. Meinel L, Hofmann S, Karageorgiou V, Zichner L, Langer R, Kaplan D, Vunjak-Novakovic G. Engineering cartilage-like tissue using human mesenchymal stem cells and silk protein scaffolds. *Biotechnology and Bioengineering* 2004;88(3):379–391. [PubMed: 15486944]
45. Weissleder R, Poss K, Wilkinson R, Zhou C, Bogdanov AA. Quantitation of slow drug release from an implantable and degradable gentamicin conjugate by in vivo magnetic resonance imaging. *Antimicrobial Agents and Chemotherapy* 1995;39:839–845. [PubMed: 7785981]
46. Sennino B, Raatschen HJ, Wendlend MF, Fu Y, You WK, Shames DM, McDonald DM, Brasch RC. Correlative dynamic contrast MRI and microscopic assessments of tumor vascularity in RIP-Tag2 transgenic mice. *Magnetic Resonance in Medicine* 2009;62:616–625. [PubMed: 19526501]

47. Cheng HLM, Wallis C, Shou Z, Farhat WA. Quantifying angiogenesis in VEGF-enhanced tissue-engineered bladder constructs by dynamic contrast-enhanced MRI using contrast agents of different molecular weights. *Journal of Magnetic Resonance Imaging* 2007;25:137–145. [PubMed: 17139634]
48. Lu ZR, Mohs AM, Zong Y, Feng Y. Polydisulfide Gd(III) chelates as biodegradable macromolecular magnetic resonance imaging contrast agents. *International Journal of Nanomedicine* 2006;1(1):31–40. [PubMed: 17722260]
49. Turetschek K, Floyd E, Helbich T, Roberts TPL, Shames DM, Wendland MF, Carter WO, Brasch RC. MRI assessment of microvascular characteristics in experimental breast tumors using a new blood pool contrast agent (MS-325) with correlations to histopathology. *Journal of Magnetic Resonance Imaging* 2001;14(3):237–242. [PubMed: 11536400]
50. Boschi F, Marzola P, Sandri M, Nicolato E, Galie M, Fiorini S, Merigo F, Lorusa V, Chaabane L, Sbarbati A. Tumor microvasculature observed using different contrast agents: a comparison between Gd-DTPA-Albumin and B-22956/1 in an experimental model of mammary carcinoma. *Magnetic Resonance in Physics, Biology, and Medicine* 2008;21(3):169–176.

**Figure 1.**

A schematic illustration of the conjugation scheme that was used to produce the protein polymer-based contrast agents. We show two examples, one for a protein polymer backbone having lysines spaced every 4 amino acids, and one in which the lysines are 8 amino acids apart.

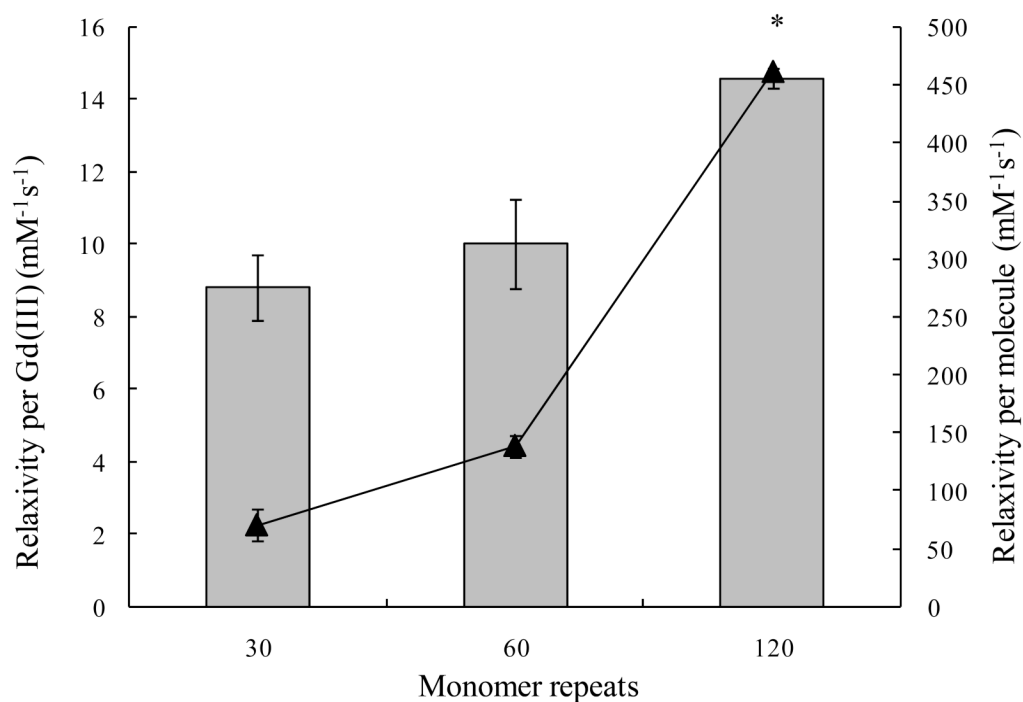


**Figure 2.** Relaxivity per Gd(III) (■) and per molecule (▲) versus number of monomer repeats. Lysines are eight amino acids apart. The relaxivity per Gd(III) of the K8-120 CA is significantly higher than that of K8-30 and K8-60 CAs. A statistically significant difference ( $P < 0.01$ ) is denoted with \*.

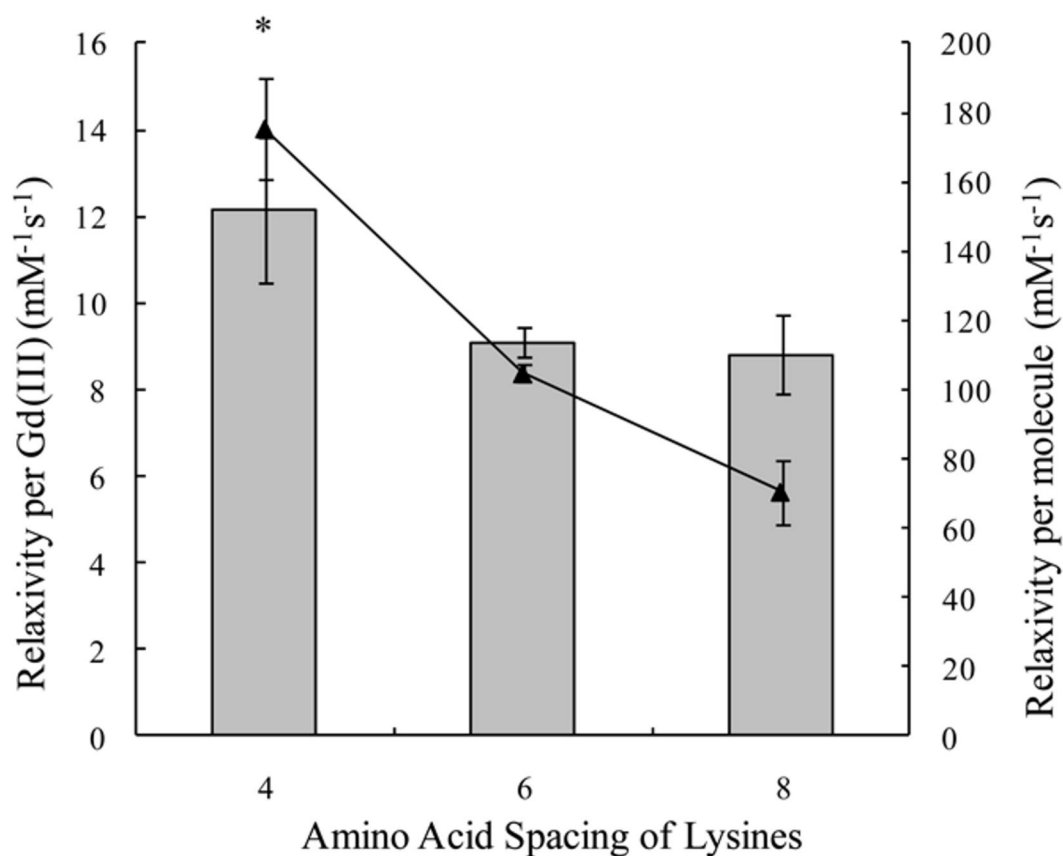


**Figure 3.** Relaxivity per Gd(III) (■) and per molecule (▲) versus lysine spacing. The molecular weight of the protein backbones is 22 kDa. The relaxivity per Gd(III) for the K4-30 CA is significantly higher than that of the K6-40 and the K8-30 CAs. A statistically significant difference ( $P < 0.01$ ) is denoted with \*.



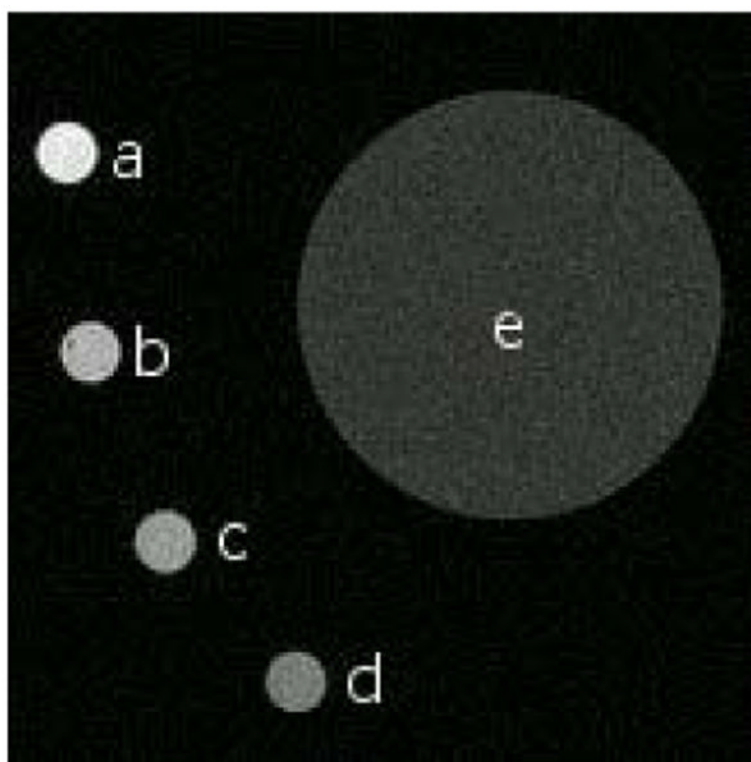


**Figure 4.** Image of K8-120 PPCA solution phantoms imaged on a 4.7 T MRI system. a) 0.37 mM Gd(III) b) 0.08 mM Gd(III) c) 0.03 mM Gd(III) d) 0.0 mM Gd(III) e) water. Gd(III) concentrations determined by ICP-MS. Imaging parameters: TR = 350 ms, TE = 14.5 ms, 4 signal averages, and a  $0.12 \times 0.12 \times 1 \text{ mm}^3$  resolution.

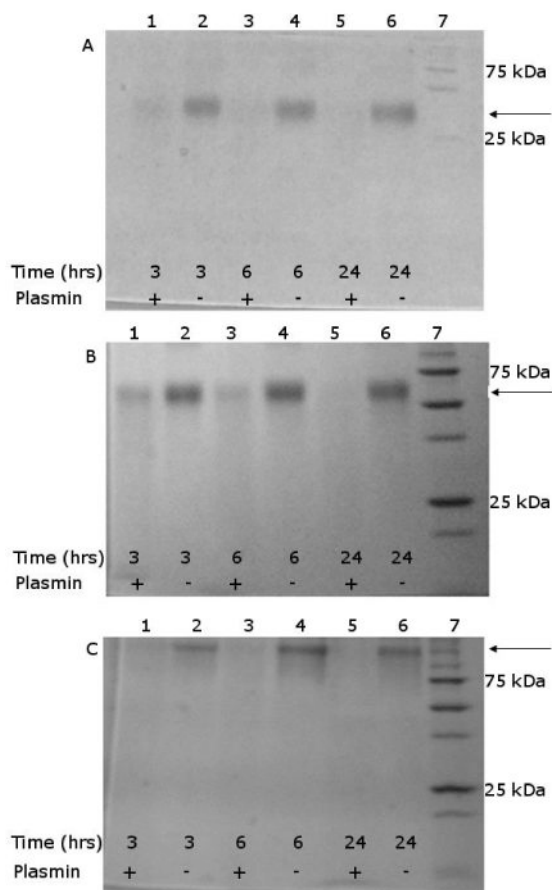


**Figure 5.** SDS-PAGE analysis of degradation by plasmin shows that the PPCAs are digested; bands for full-molar mass protein decrease in intensity over time, when plasmin is present. A) K8-30 B) K8-60 and C) K8-120 PPCA. In A, B, and C, Lane 1: (+) plasmin, 3 hours; Lane 2: (-) plasmin, 3 hours; Lane 3: (+) plasmin, 6 hours; Lane 4: (-) plasmin, 6 hours; Lane 5: (+) plasmin, 24 hours; Lane 6: (-) plasmin, 24 hours; Lane 7: molecular weight marker. Arrows mark the peak with the full PPCA molar mass.

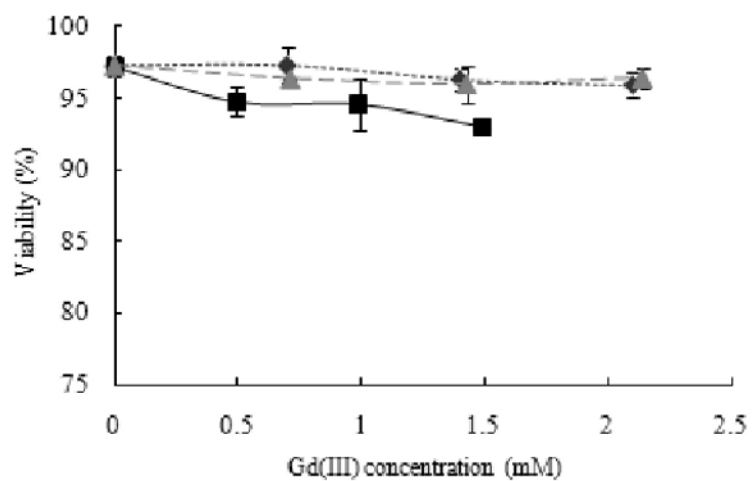


**Figure 6.** Cell viability of MIN6 cells after incubated for 5 hours with K8-30 CA (◆), K8-60 CA (■), and K8-120 CA (▲), all with lysines spaced eight amino acids apart. Viability is between 92 and 97% for all three PPCAs.

**Table 1**  
**Protein Polymer Contrast Agent Properties with Varying Number of Monomer Repeats and Lysines Spaced Every 8 Amino Acids**

	<b>K8-30</b>	<b>K8-60</b>	<b>K8-120</b>
Average # of Gd(III) per molecule	8.0	14	32
# of Lysines per protein	31	61	121
Protein molar mass (kDa)	21.7	40.6	78.4
Conjugation efficiency (%)	27	23	26
Relaxivity per Gd(III) ( $\text{mM}^{-1}\text{s}^{-1}$ )	8.8	10.0	14.6
Relaxivity per molecule ( $\text{mM}^{-1}\text{s}^{-1}$ )	70.5	138.9	461.4

**Table 2**  
**Protein Polymer Contrast Agent Properties with Varying Lysine Spacing and Molecular Weight of 22 kDa**

	<b>K4-30</b>	<b>K6-40</b>	<b>K8-30</b>
Average # of Gd(III) per molecule	14.5	11.5	8.0
# of Lysines per protein	61	41	31
Protein molar mass (kDa)	22.1	21.7	21.7
Conjugation efficiency (%)	23.9	28.0	26.7
Relaxivity per Gd(III) ( $\text{mM}^{-1}\text{s}^{-1}$ )	12.1	9.1	8.8
Relaxivity per molecule ( $\text{mM}^{-1}\text{s}^{-1}$ )	175.4	104.7	70.5

**Table 3**  
**T<sub>1</sub> and T<sub>2</sub> Values of Phantoms at 4.7 T**

Concentration (mM Gd(III))	T <sub>1</sub> (ms)	T <sub>2</sub> (ms)	T <sub>1</sub> /T <sub>2</sub>
0.37	382.9 +/- 24.5	43.0 +/- 2.5	8.9
0.08	747.2 +/- 37.1	69.1 +/- 3.5	10.8
0.03	899.1 +/- 40.4	86.0 +/- 3.8	10.5
0.00	1270.4 +/- 39.5	116.8 +/- 6.0	10.9